Int. J. Electrochem. Sci., 13 **(2018)** 6771 – 6778, 10.20964/2018.07.36

International Journal of
ELECTROCHEMICAL
SCIENCE
www.electrochemsci.org

Precursor-template Strategy toward Hollow Nanostructured $Li(Ni_{1/3}Co_{1/3}Mn_{1/3})O_2$ Microspheres Cathode with Enhanced Electrochemical Performance

Zhenya Kang, Yourong Wang[*]*, Mengzhi Yao and Siqing Cheng*[*]

Innovation Center for Nanomaterials in Energy and Medicine (ICNEM), School of Chemical and Environmental Engineering, Wuhan Polytechnic University, Hubei 430023, P. R. China
[*]E-mail: chengsqing@iccas.ac.cn

Received: 14 March 2018 / *Accepted:* 8 May 2018 / *Published:* 5 June 2018

The hollow nanostructured $Li(Ni_{1/3}Co_{1/3}Mn_{1/3})O_2$ (NCM) microspheres with low Li/Ni disorder were fabricated by precursor-template approach and investigated electrochemically as lithium ion batteries (LIBs) cathode. The as-obtained NCM microspheres cathode exhibits high specific capacity, good coulombic efficiency and outstanding rate capability. This might mainly be due to the unique hollow nanostructured architectures of the NCM microspheres enabling to shorten Li^+ diffusion and electron transportation paths in the materials, which is verified via the cyclic voltammetry (CV) at various scan rate to obtain the high apparent Li^+ diffusion coefficient for the discharge/charge processes.

Keywords: $Li(Ni_{1/3}Co_{1/3}Mn_{1/3})O_2$ (NCM); Precursor template; cathode materials; Lithium ion batteries (LIBs); Electrochemical performance.

1. INTRODUCTION

With ever-increasing concern about resources and the environmental issues owing to the rapid development of intelligent and mechanized industry, the intermittent energy conversion and storage technology based on lithium-ion batteries (LIBs) with high energy and power densities has aroused considerable attention.[1-4] Nevertheless, the further implementation of LIBs has been impeded mainly due to these often used cathode materials such as $LiCoO_2$, $LiMn_2O_4$, $LiFePO_4$ etc. in view of their reversible specific capacity, cost, toxicity and safety.[5-8] As such, extensive investigation has been directed to the fabrication and optimization of alternative cathode materials of LIBs. Among these cathode materials, layered $Li(Ni_{1/3}Co_{1/3}Mn_{1/3})O_2$ (NCM) has been demonstrated potential as alternative to those widely used cathode materials such as $LiCoO_2$, $LiMn_2O_4$, $LiFePO_4$ in light of its

superior comprehensive properties of low toxicity and cost, high reversible capacity and energy density, excellent thermal stability, appropriate voltage platform.[9-11] Notwithstanding numerous implementations in many studies and even in some commercial application, there still exist some dominating defects of the NCM to deteriorate their electrochemical performance of rate capability and cycling performance, restricting their enduring and high-efficient practical applications, including low electronic conductivity due to the substitution of Co by Ni and Mn, and limited Li-ion movement due to Li/Ni disorder.[12-15]

To solve these issues, various synthetic approaches such as co-precipitation method [16, 17], sol-gel method[18-20], glycine-nitrate combustion[21], molten salt[22], pyrolysis process [23, 24] etc. have been utilized to prepared high quality of NCM powders with uniform morphology and small particle size to ameliorate the cationic disordering with the present of Ni in the Li-site, yielding good rate capability and cycling performance. On the other hand, the fabrication of nanostructured NCM with hollow morphology has been deemed to be an effective strategy in order to improve the electrical conductivity, which is due to the unique architecture being capable of affording the shorter Li^+ diffusion path and the larger contact area with electrolyte, resulting in high specific capacity and thus high energy and powder density.[25, 26] Therefore, it is highly desirable to develop an appropriate synthesis approach to fabricate the hollow nanostructured architecture of NCM without cationic disordering, which still remains a great challenge.

The sacrificial template strategy [26, 27] has been regarded as a ripe method to construct hollow nanostructures with its many advantages such as easy-to–operation, scalable production. However, the sacrificed template might contaminate the ultimate products and thus influence the performance. Herein, we have demonstrated the facilely prepared hollow precursor $Mn_{1.5}Co_{1.5}O_4$ as a template to fabricate the hollow nanostructured NCM microspheres without any other component to be introduced. The as-obtained products were investigated electrochemically to achieve high rate capability and excellent cycling performance.

2. EXPERIMENTAL SECTION

All chemicals in this experiment were purchased from Sinopharm Chemical Reagent Co., Ltd., Shanghai and used directly without further purification unless otherwise stated. Deionized double-distilled water was used. The hollow nanostructured NCM were synthesized from its precursor $Mn_{0.5}Co_{0.5}CO_3$ microspheres as template. In a typical experiment, 1.5 mmol Co $(CH_3COO)_2 \cdot 4H_2O$ (99%, AR) and 1.5 mmol $Mn(CH_3COO)_2 \cdot 4H_2O$ (99%, AR) were dissolved completely in 40 mL of glycol under vigorous stirring and then 30 mmol of NH_4HCO_3 was added into the above mixed solution to form a homogeneous deep purple solution. The resultant mixed solution was transferred to a 50 mL Teflon-lined stainless steel autoclave and maintained in the oven at 200 ℃ for 20 h. The obtained pink precipitation was separated by centrifugation, alternately washed many times with deionized double-distilled water and ethanol, and dried overnight at 60 ℃ in a vacuum oven to remove water, yielding the pink $Mn_{0.5}Co_{0.5}CO_3$ microspheres. Subsequently, the obtained $Mn_{0.5}Co_{0.5}CO_3$ microspheres were calcined at 400 ℃ for 10 h in a muffle furnace with a heating rate of 4℃/min to

yield hollow black $Mn_{1.5}Co_{1.5}O_4$ microspheres. Eventually, the mixture of $LiOH{\cdot}4H_2O$, $Ni(NO_3)_2{\cdot}6H_2O$ and the product $Mn_{1.5}Co_{1.5}O_4$ with molar ratio of 1.07:0.33:0.22 was dispersed in absolute ethanol and then evaporated naturally under continuous stirring. The resulting homogenous solid mixture was ground and then calcined at 900 ℃ for 10 h in a muffle furnace with a heating rate of 1.5 ℃/min to generate the hollow nanostructured NCM microspheres.

The phase structures of the as-prepared samples were characterized by powder X-ray diffraction (XRD) on a Shimadzu DX-7000 advanced X-ray diffraction operated at 40 kV and 40 mA using Cu Kα radiation (λ = 0.154 nm) over 2θ degree from 10° to 70° at a scan rate of 4° min^{-1}. A Hitachi scanning electron microscopy (SEM) was employed to observe the morphologies and microstructures of the as-prepared NCM microspheres. The inductively coupled plasma-optical emission spectrometer (ICP-OES) was used to determine the chemical component of the NCM microspheres. The cyclic voltammetry (CV) measurements were performed in two-electrode cells on a CHI660B electrochemical workstation (Chenghua, Shanghai, China) over a potential voltage of 2.5-4.6 V (vs. Li/Li^+) at various scan rates.

The as-prepared NCM microspheres cathode were assembled using the doctor blade technique by pasting the slurries of the as-prepared NCM microspheres (80 wt%) as active materials, acetylene black (10 wt%) as conductive agent and polyvinylidene difluoride (PVDF, 10 wt%)) as binding agent dissolved in N-methylpyrrolidone (NMP) on aluminum foil. Then, the obtained cathode sheets were dried at 60℃ for 12 h in a vacuum oven. The electrolyte was 1 M $LiPF_6$ dissolved in ethylene carbonate (EC) and diethyl carbonate (DEC) (1:1 by volume) solvent mixture. CelgardR 2325 was used as separator. Consequently, CR2016 coin-type cells with lithium metal foil as the anode were assembled in a glove box filled with high-purity argon. The electrochemical performance tests were executed on a program-controlled Battery Test System (Land®, Wuhan, China) between 2.5 and 4.6 V (vs. Li/Li^+) at various current rates at ambient temperature.

3. RESULTS AND DISCUSSION

In order to prepare hollow nanostructured NCM microspheres, the easily obtained carbonate $Mn_{0.5}Co_{0.5}CO_3$ is acted as initial reactant to be calcined to yield hollow $Mn_{1.5}Co_{1.5}O_4$ template due to the release of CO_2 as well as Mn and Co sources. Subsequently, the introduction of lithium hydroxide and nickel nitrate by impregnation could retain the morphological and structural integrity of hollow $Mn_{1.5}Co_{1.5}O_4$ template through the calcinations of high temperature at 900 ℃. Fig. 1 presents the SEM images from the precursor to the as-obtained NCM microspheres and the powder X-ray diffraction (XRD) pattern of the as-obtained NCM microsphere. From the SEM images of Fig.1a-c, it is obvious that the morphology and structure is kept integrity from the precursor to the desirable NCM microspheres. Specially, Fig. 1c demonstrates the intact hollow nanostructured NCM microspheres of no agglomeration with uniform particle size of ca. 150 nm in diameter, as marked by red hollow cycle, which is very favorable for the improvement of electrochemical performance. On the other hand, the narrow distribution of the pore size with about 2 nm in diameter is considerably beneficial for the subsequent electrochemical reaction due to the impregnation of Ni, Co and Li ions. The phase

composition and crystal structure of the as-prepared NCM microspheres were identified by the powder X-ray diffraction (XRD), as displayed in Fig.1d. All XRD reflections are well fitted to a pure hexagonal a-$NaFeO_2$ type structure with a space group of R-3m, with no extra impurity peaks being found. All incisive diffraction peaks are observed in the XRD pattern, indicative of good crystallinity.[28] The calculated lattice constants of the NCM microspheres by the least-square method[29] are to a=2.8652 Å, b=2.8652 Å, c=14.2750 Å with high c/a value of 4.98, while the obvious splitting of (006)/(012) peaks and (108)/(110) peaks are clearly identified, revealing the well-defined hexagonal layered structure of the as-prepared NCM microspheres. The intensity ratio of (003)/(104) is determined to be ca. 1.30, confirming the low degree of Ni^{2+}/Li^{+} cation mixing in the as-prepared NCM microspheres.[30] The determined ingredient of the as-prepared NCM microspheres by ICP analysis is 1:0.32:0.31:0.33 (molar ratio) of Li:Ni:Co:Mn, yielding the corresponding chemical formula of $Li(Ni_{1/3}Co_{1/3}Mn_{1/3})O_2$. Therefore, the precursor-template method used for the synthesis of hollow nanostructured NCM microsphere is feasible.

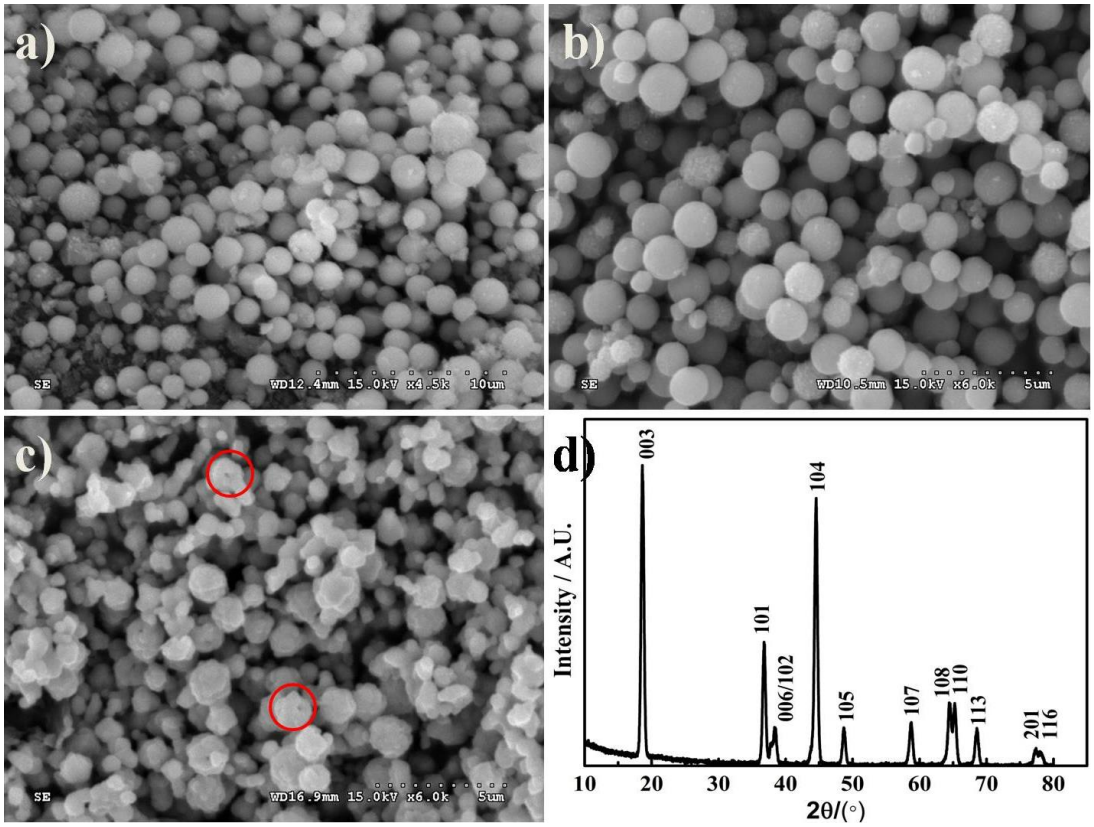

Figure 1. SEM images for $Mn_{0.5}Co_{0.5}CO_3$ (a), $Mn_{1.5}Co_{1.5}O_4$ (b) and NCM microspheres (c) and XRD pattern for the as-obtained NCM microspheres (d).

Fig. 2a presents the galvanostatic discharge-charge curves for the first four cycles at a current rate of 300 mA g^{-1} in the voltage range of 2.5 V - 4.6 V versus Li/Li^{+}. The specific discharged capacities for the first four cycles at a current rate of 300 mA g^{-1} are 167.7, 164.9, 162.8, 160.9 mA h g^{-1}, respectively, which are comparable to those of the materials previously reported in the literatures[26, 31]. The charged specific capacities for the first four cycles are 198.0, 168.9, 165.6,

163.4 mAh g^{-1}, respectively. Thus, the corresponding Coulombic efficiency for the first four cycles are 84.7%, 97.6%, 98.3%, 98.5%, respectively. The initial less coulombic efficiency might be mainly due to the formation of a solid electrolyte interface (SEI) and electrolyte decomposition.[25] The stable plateau in the curves indicate the stability of the structure of the as-obtained NCM microsphere when charged/discharged, revealing the excellent cycling performance.

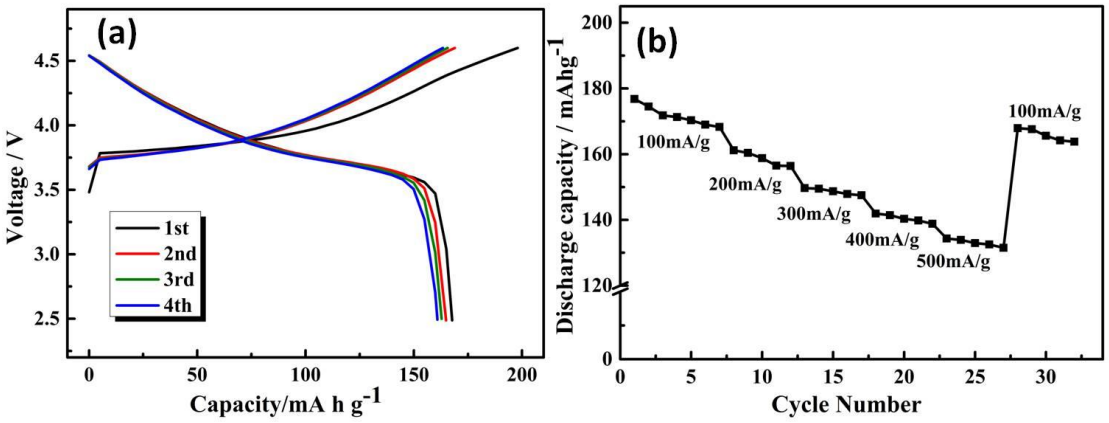

Figure 2. Electrochemical performance of the as-obtained hollow nanostructured NCM microspheres cathode: (a) Galvanostatic discharge /charge curves in the voltage range of 2.5-4.6 V versus Li/Li^+ at a current rate of 300 mA g^{-1}; (b) rate capability at different current densities.

The rate capability of the as-prepared NCM microspherical cathode between 2.5 and 4.6 V at various current densities is displayed in Fig.2b. The cathode is charged and discharged galvanostatically at ambient temperature with sequential current densities of 100 mA g^{-1}, 200 mA g^{-1}, 300 mA g^{-1}, 400 mA g^{-1}, 500 mA g^{-1}, ultimately returning to 100 mA g^{-1}, respectively. The high maximal discharge capacities of 176.8, 166.2, 149.7, 141.9 mAh g^{-1} are achieved at current rates of 100 mA g^{-1}, 200 mA g^{-1}, 300 mA g^{-1}, 400 mA g^{-1}, 500 mA g^{-1}, respectively. This result might be attributed to the unique porous interior of the as-prepared NCM microsphere, which could accommodate the large volume expansion even from rapid Li^+ diffusion at high current rate. It is worth noting that the discharge specific capacity is retained at 95% after the current rate returned to 100 mA g^{-1}, indicating the good rate capability and thus the high electronic conductivity and Li^+ diffusion.

Fig.3 demonstrates the first four cyclic voltammetry profiles of the as-obtained NCM microsphere cathode at a scan rate of 0.1 mV s^{-1} within the potential range of 2.5-4.6 V vs. Li/Li^+. There is a sharp oxidation (cathodic or lithiation) peak at 3.9 V, corresponding to the reduction (anodic or delithiation) peak at 3.7 V, which is ascribed to the redox reaction of Ni^{2+}/Ni^{4+}. However, no redox peaks of the Co^{3+}/Co^{4+} couple within the investigated potential range could be observed due to the redox potential of greater than 4.6 V. Also, the redox peaks of Mn^{3+}/Mn^{4+} at 3.0 V are not observed, revealing the electrochemical inactiveness of Mn. After the first cycle, the CV curves in the sequent cycles almost show the same trace, indicating good reversibility of lithiation/delithiation process. Herein, it is worth noting that the narrow potential interval of 0.2 V between the cathodic and anodic peaks exhibits the low polarization of electrode, indicating the fast reaction kinetics of Li^+ diffusion

and charge transfer in the NCM microsphere cathode[32], which is also analyzed via the CVs at various scan rates, as displayed in Fig.4a.

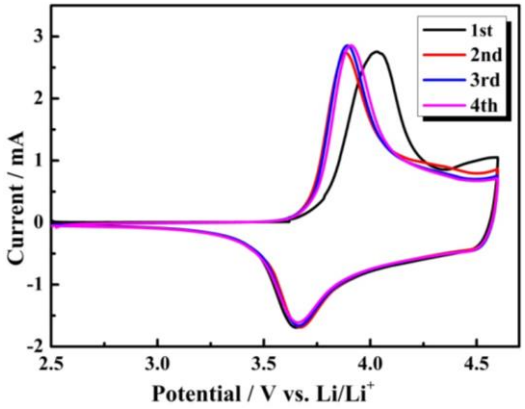

Figure 3. The first four consecutive cyclic voltammetric curves at a scan rate of 0.1 mV s^{-1} in the voltage range of 2.5-4.6 V versus Li/Li^+.

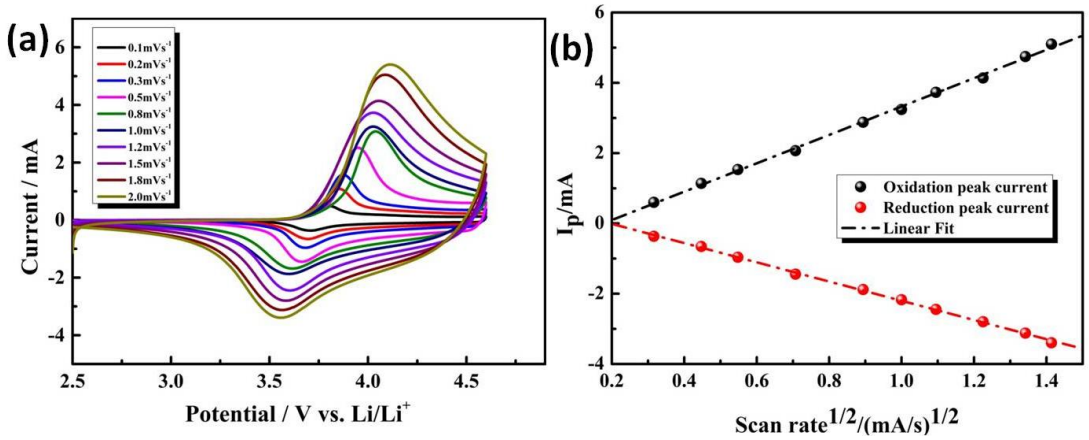

Figure 4. (a) cyclic voltammetric curves at different scan rates; (b) the linear relationship of the peak current intensity as a function of the square root of scan rate.

From the shift tendency of reduction and oxidation peak with increasing the scan rate, it is indicated that the electrode reaction of the as-obtained NCM microsphere material is controlled by diffusion[33]. Fig.4b illustrates the linear relationship between the reduction or oxidation peak current intensity and the square root of the scan rate. Thus, the apparent Li^+ diffusion coefficients of the as-obtained NCM microsphere electrode for oxidation and reduction processes could be calculated based on the Randles-Sevcik equation [34, 35]:

$$I_p = 2.69 \times 10^5 n^{3/2} A D^{1/2} C v^{1/2} \quad (1)$$

where I_p is the peak current intensity in A, n is the number of electrons transferred per reaction molecule, A is the electrode surface area in cm^2, D is the apparent Li^+ diffusion coefficient in $cm^2\ s^{-1}$, C is the Li^+ molar concentration in mol cm^{-3}, v is the scan rate in mV s^{-1}. From the slope of the fitted line of Fig. 4b, the apparent diffusion coefficients of lithium ions for oxidation and reduction processes are 2.986×10^{-9} and 6.762×10^{-10} $cm^2\ s^{-1}$, respectively, which is comparable to the reported results [36].

This further manifests that the hollow nanostructure facilitates the rapid Li^+ diffusion and fast charge transfer in the as-obtained NCM microspheres.

4. CONCLUSIONS

Overall, the hollow nanostructured NCM mcirospheres with low Li/Ni disorder were synthesized successfully by precursor-template method without any contaminant and investigated electrochemically as high performance LIBs cathode materials. The as-obtained NCM cathode delivers an initial discharge specific capacity of as high as 167 mA h g^{-1} at a current density of 300 mA g^{-1} and presents a high coulombic efficiency of more than 95% after the first cycle. Specially, the outstanding rate capability of the as-obtained NCM cathode is achieved with an initial discharge capacity retention of more than 95%. All these good electrochemical performance might be ascribed to the unique hollow nanostructured architecture enabling to generate short lithium ions diffusion and electron transportation paths, which is verified by the cyclic voltammetry at various scan rate to obtain the high apparent Li^+ diffusion coefficient of 2.986×10^{-9} cm^2 s^{-1} for the discharge process.

ACKNOWLEDGEMENTS
This work was supported by the Hubei Provincial Natural Science Foundation of China (No. 2015CFC842) and by the Education Science Foundation of Hubei Province (No. T200908).

References

1. W. Li, B. Song and A. Manthiram, *Chem. Soc. Rev*., 46 (2017) 3006.
2. X. Lin, M. Salari, L. M. Arava, P. M. Ajayan and M. W. Grinstaff, *Chem. Soc. Rev*., 45 (2016) 5848.
3. G. Zhou, F. Li and H.-M. Cheng, *Energy Environ. Sci*., 7 (2014) 1307.
4. M. Armand and J. M. Tarascon, *Nature*, 451 (2008) 652.
5. E. Antolini, *Solid State Ion*., 170 (2004) 159.
6. H. Porthault, F. Le Cras and S. Franger, *J. Power Sources*, 195 (2010) 6262.
7. H. Xia, Z. T. Luo and J. P. Xie, *Prog. Nat. Sci. Mater*., 22 (2012) 572.
8. T. F. Yi, X. Y. Li, H. P. Liu, J. Shu, Y. R. Zhu and R. S. Zhu, *Ionics*, 18 (2012) 529.
9. X. Y. Han, Q. F. Meng, T. L. Sun and J. T. Sun, *J. Power Sources*, 195 (2010) 3047.
10. C. X. Tian, F. Lin and M. M. Doeff, *Acc. Chem. Res*., 51 (2018) 89.
11. K. Zaghib, A. Mauger, H. Groult, J. B. Goodenough and C. M. Julien, *Materials*, 6 (2013) 1028.
12. F. Li, G. Yang, G. Jia, X. Shangguan, Z. Qin and B. Bai, *J. Appl. Electrochem*., (2017) 1.
13. M. Chennabasappa, B. Kelly, D. Bender, J. Garrett and M. Venkatesan, *Int. J. Hydrogen Energy*, 43 (2018) 4101.
14. C. Tian, F. Lin and M. M. Doeff, *Acc. Chem. Res*., 51 (2018) 89.
15. J. Zeng, C. Hai, X. Ren, X. Li, Y. Shen, O. Dong, L. Zhang, Y. Sun, L. Ma, X. Zhang, S. Dong and Y. Zhou, *J. Alloys Compd*., 735 (2018) 1977.
16. R. Santhanam and B. Rambabu, *J. Power Sources*, 195 (2010) 4313.
17. S. Zhang, C. Deng, B. L. Fu, S. Y. Yang and L. Ma, *Powder Technol*., 198 (2010) 373.
18. C. H. Chen, C. J. Wang and B. J. Hwang, *J. Power Sources*, 146 (2005) 626.

19. N. Kiziltas-Yavuz, M. Herklotz, A. M. Hashem, H. M. Abuzeid, B. Schwarz, H. Ehrenberg, A. Mauger and C. M. Julien, *Electrochim. Acta*, 113 (2013) 313.
20. Q. Qiu, X. Huang, Y. M. Chen, Y. Tan and W. Z. Lv, *Ceram. Int*., 40 (2014) 10511.
21. T. Amaraweera, A. Wijayasinghe, B. E. Mellander and M. Dissanayake, *Ionics*, 23 (2017) 3001.
22. M. V. Reddy, G. V. S. Rao and B. V. R. Chowdari, *J. Power Sources*, 159 (2006) 263.
23. R. Guo, P. F. Shi, X. Q. Cheng and C. Y. Du, *J. Alloys Compd*., 473 (2009) 53.
24. H. C. Wu, Z. Z. Guo, M. H. Yang, C. H. Lu, T. Y. Wu and I. Taniguchi, *Chem. Lett*., 34 (2005) 1398.
25. X. Li, X. Zhao, M.-S. Wang, K.-J. Zhang, Y. Huang, M.-Z. Qu, Z.-L. Yu, D.-S. Geng, W.-G. Zhao and J.-M. Zheng, *RSC Adv*., 7 (2017) 24359.
26. Y. Zhang, W. Zhang, S. Shen, X. Yan, R. Wu, A. Wu, C. Lastoskie and J. Zhang, ACS Omega, 2 (2017) 7593.
27. J. P. Liu, Y. Y. Li, H. J. Fan, Z. H. Zhu, J. Jiang, R. M. Ding, Y. Y. Hu and X. T. Huang, *Chem. Mater.*, 22 (2010) 212.
28. J. Li, S. Xiong, Y. Liu, Z. Ju and Y. Qian, *Nano Energy*, 2 (2013) 1249.
29. H. Lu, H. Zhou, A. M. Svensson, A. Fossdal, E. Sheridan, S. Lu and F. Vullum-Bruer, *Solid State Ion.*, 249-250 (2013) 105.
30. Z. Chen, J. Wang, D. Chao, T. Baikie, L. Bai, S. Chen, Y. Zhao, T. C. Sum, J. Lin and Z. Shen, *Sci. Rep.*, 6 (2016) 25771.
31. Z. Chen, J. Wang, D. Chao, T. Baikie, L. Bai, S. Chen, Y. Zhao, T. C. Sum, J. Lin and Z. Shen, *Sci Rep*, 6 (2016) 25771.
32. J. M. Lim, D. Kim, M. S. Park, M. Cho and K. Cho, *Phys Chem Chem Phys*, 18 (2016) 11411.
33. H. Xia, L. Lu and M. O. Lai, *Electrochim. Acta*, 54 (2009) 5986.
34. M. C. Henstridge, E. Laborda, E. J. F. Dickinson and R. G. Compton, *J. Electroanal. Chem*., 664 (2012) 73.
35. R. E. Sioda and B. Frankowska, *J. Electroanal. Chem*., 612 (2008) 147.
36. L. Peng, Y. Zhu, U. Khakoo, D. Chen and G. Yu, *Nano Energy*, 17 (2015) 36.